

Polyolefin-Clay Nanocomposites from Olefin Polymerization between Clay Layers

Jinhua Qian^a and Cun-Yue Guo^{*b}

^aScience, Technology & Information Management Department, PetroChina Company Limited, Beijing 100011, P. R. China

^bBeijing National Laboratory for Molecular Sciences (BNLMS), Laboratory of New Materials, Institute of Chemistry, Chinese Academy of Sciences, Beijing 100190, P. R. China

Abstract: This mini-review article addresses the development in synthesizing polyolefin/clay nanocomposites by olefin polymerization under catalysis of clay intercalated precatalysts in recent years. The review comprises three parts which focus on mainly the synthetic route, structural characterization, and properties of polyolefin/clay nanocomposites, respectively. Moreover, outlook for future research and development trends is outlined.

Keywords: Polyolefin/clay, nanocomposites, polymerization, outlook.

INTRODUCTION

Polyethylene and polypropylene occupy about half the total production capacity in synthetic plastics. Having been an important field in both academy and industry for more than half century [1], polyolefin nanocomposites are still attracting interests from numerous researchers due to their superior properties such as strong interfacial interaction between inorganic fillers and organic polymers, improved onset decomposition temperatures (T_{onset}), heat distortion temperatures (HDT), increased mechanical properties, excellent impermeability to small molecules as H_2O and CO_2 , good nonflammability, and better dyeability, etc. with a small amount of fillers (usually < 5 wt %). Significant advancements in polyolefin/clay nanocomposites have been accomplished since the successful preparation of nylon 6/clay in late 1980s [2]. Clay includes mainly montmorillonite (MMT), hectorite, and saponite, etc (Table 1). The great polarity discrepancy between polyolefins and clay makes the manufacture of polyolefin/clay nanocomposites a great challenge. Up to now, three types of methods have been developed to prepare polyolefin/clay nanocomposites. The first is melt intercalation compounding in which the polyolefins, modified clay, and additives were extruded together above the melting temperatures of polyolefins to form intercalated or exfoliated polyolefin/clay nanocomposites [3-7]. The second is solution blending in which an organic-modified clay was dispersed in polyolefin resin dissolved in an organic solvent to form intercalated polyolefin/clay nanocomposite [8-11]. The last yet the most promising strategy receiving greatly increasing attention involves a silicate that was intercalated by an initiator or catalyst [12-42], and, upon the introduction of monomers, an intercalated or exfoliated polymer nanocomposite was formed. Besides cases of conducting

ethylene homopolymerization, there have been reports about the synthesis of polyethylene/montmorillonite (PE/MMT) nanocomposites by copolymerization of ethylene with *in situ* produced α -olefins under a dual functional catalyst system intercalated into MMT layer [23, 24, 35, 38]. The present review will present the most recent progress in polyolefins (predominantly polyethylene (PE) and polypropylene (PP))/clay nanocomposites (PE/MMT and PP/MMT, respectively) relating to their synthetic routes, structural characterization, and property investigation.

1. Synthesis of Polyolefin/Clay Nanocomposites

The preparation of polyolefin/clay nanocomposites from olefin polymerization is essentially the same although four types of catalysts including Ziegler-Natta catalysts [12-22], metallocene catalysts [23-38], non-metallocene catalysts [39], and late transition metal (LTM) catalysts [40-42] are used. To achieve uniform dispersion of clay layers throughout polyolefin matrix, the key factor is the immobilization of precatalysts onto clay. It is the exotherm released from olefin polymerization plus propagating polyolefin chains that exfoliate and disperse the clay layers. Polymerization-induced formation of polyolefin/clay nanocomposites is advantageous in that 1) unfavorable thermodynamic requirement for melt intercalation is avoided; 2) facile adjustment of clay loading and the accompanying nanocomposites' properties; 3) no special demand on polyolefin molecular weights and no need of introducing olefin oligomer modifiers; 4) more homogeneous dispersion of clay layers in the polymeric matrix.

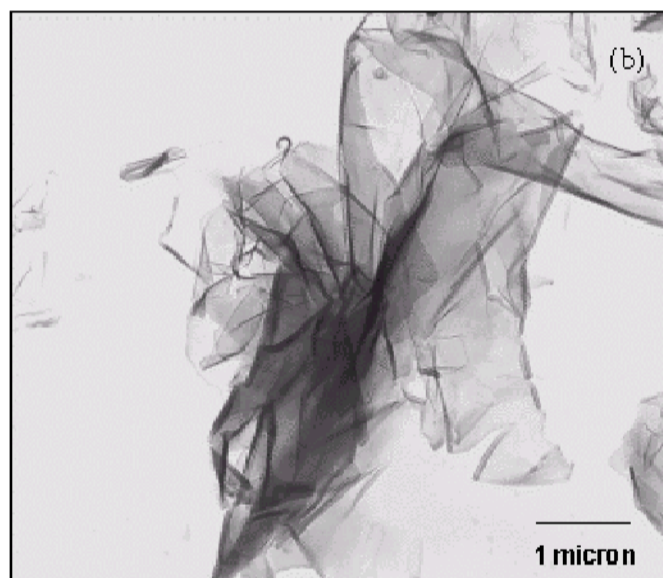
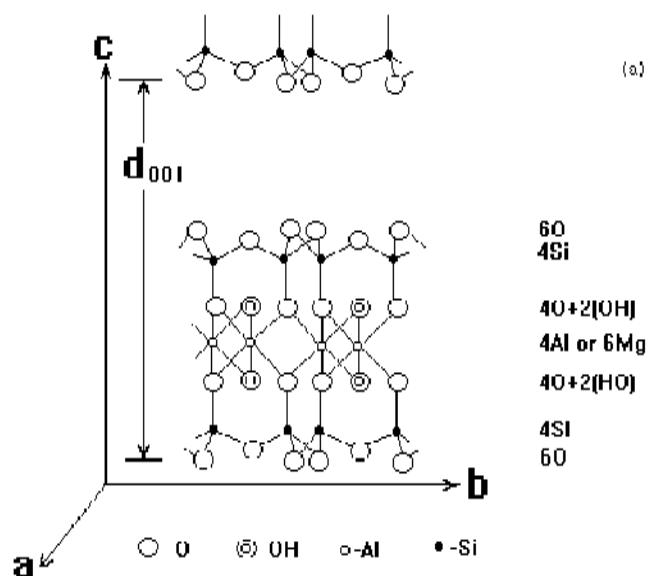
Now that MMT (Scheme 1) is used most extensively for research and development, it is convenient thereafter to focus on MMT in elucidating the whole process of producing polyolefin/MMT (POE/MMT) nanocomposites. The key issue in immobilizing olefin polymerization catalysts onto MMT is that the high polarity arising from MMT's surface groups and the resultant complicated physical and chemical properties lower the polymerization activities of almost all

*Address correspondence to this author at the Beijing National Laboratory for Molecular Sciences (BNLMS), Laboratory of New Materials, Institute of Chemistry, Chinese Academy of Sciences, Beijing 100190, P. R. China; Tel: +86-10-62560247; Fax: +86-10-62559373; E-mail: cyguo@iccas.ac.cn

Table 1. Chemical Composition and Parameters of Clay (2:1 Type)

Clay	Chemical composition ^a	CEC (mequiv/100 g)	Particle size (nm)
MMT	$M_x(Al_{4-x}Mg_x)Si_8O_{20}(OH)_4$	110	100-50
Hectorite	$M_x(Mg_{6-x}Li_x)Si_8O_{20}(OH)_4$	120	200-300
Saponite	$M_xMg_6(Si_{8-x}Al_x)Si_8O_{20}(OH)_4$	86.6	50-60

^aM = monovalent metal cation; x = 0.5-1.3.



Scheme 1. Schematic structure of MMT (a); and TEM image of MMT (b).

catalysts. Such that a series of treatment is necessary to synthesize POE/MMT nanocomposites as exemplified in Fig. (1) [42].

The first step is the formation of organo MMT (OMMT). The purpose of this treatment is reducing the surface energy of MMT, increasing the interlayer spacing of MMT, and creating anchoring points for catalyst incorporation. In most cases, this can be realized by ion exchanging of MMT with organic amines that preliminarily increased the interlayer spacing of MMT ($d_{001} = 1.99$ nm). The second step is the immobilization of (pre)catalysts for olefin polymerization that further expanded this distance ($d_{001} = 2.76$ nm). The last step finalizing the formation of the nanocomposite is olefin polymerization between layers of MMT. As time went on the d_{001} values increased gradually and the structure of the nanocomposites evolves from intercalation ($d_{001} = 3.27$ nm) to exfoliation (no characteristic diffraction peak of MMT observed) accordingly.

As the first example attempting POE/MMT nanocomposite fabrication [12], the treatment of Li-MMT with methylaluminumoxane (MAO) did not increase the d_{001} value (0.96 nm). However, the immobilization of $[Zr(\eta-C_5H_5Me(thf))BPh_4]$ ($d_{001} = 1.44$ nm) via ion exchanging with Na^+ afforded active species towards propylene polymerization and formed PP/MMT nanocomposite (Fig. 2). Grounding together OMMT and $MgCl_2$ offered support for $TiCl_4$ that, upon activation with triethylaluminum (TEA), polymer-

ized propylene to intercalated PP/MMT nanocomposites [15].

To improve the supporting efficiency of metallocene complex, amine compound capable of activating metallocene was ion exchanged with MMT and employed in successful production of exfoliated PP/MMT nanocomposite with high activity (26×10^6 g PP (mol metal h)⁻¹) [26].

MMT after exchanged with positively charged stearyl trimethyl ammonium chloride can support *rac*-Et(Ind)₂ZrCl₂ in forming partially exfoliated PP/MMT nanocomposite [33]. Monoalkylimidazolium- [18] or alkyltriphenylphosphonium-modified MMT [19] was useful to form $TiCl_4/MgCl_2/MMT$ compound catalyst and produced exfoliated PP/MMT nanocomposites through intercalative polymerization of propylene although the MMT loadings are only about 2.0 wt %.

Metallocene catalysts constitute majority of all the polymerization-generated PE/MMT nanocomposites [23-25, 27-32, 34-36, 38] whereas there is little research relating to PP/MMT nanocomposites when metallocene catalysts were adopted [26, 33, 37]. Four types of metallocene complexes were immobilized onto MMT and exhibited catalytic activities towards ethylene polymerization [25]. Na^+ -MMT and Cloisite 25A exerted different efficiencies in immobilizing Cp_2ZrCl_2 , only the OMMT support achieved high ethylene polymerization activities and formed exfoliated nanocomposites [32]. Various modifiers like $[CH_3O_2CCH_2NH_3]^+$

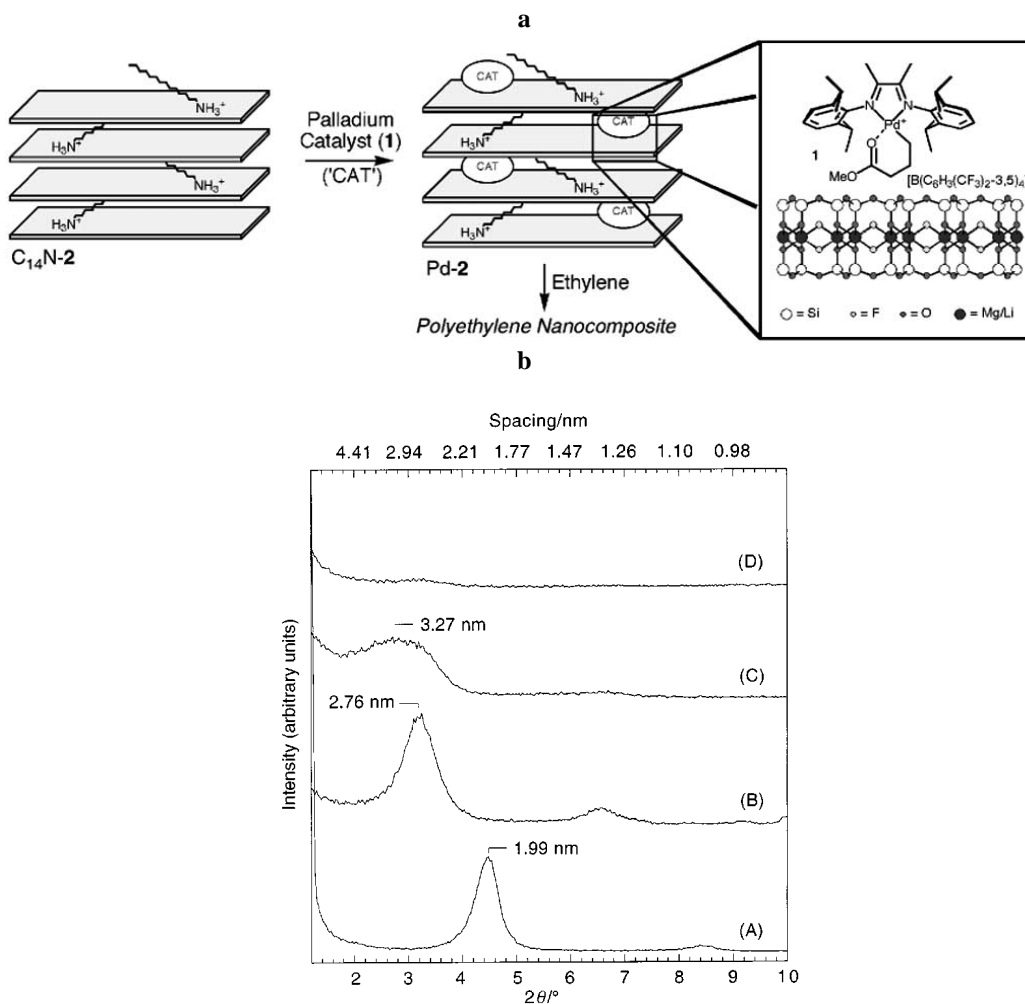


Fig. (1). (a) Formation of PE/MMT nanocomposites using a Brookhart's single component palladium-based complex; (b) XRD patterns: (A) 1-tetradecylammonium modified fluorohectorite (C₁₄N-2); (B) C₁₄N-2 after intercalation by 1 (Pd-2); (C) Pd-2 after exposure to ethylene for 135 min; (D) Pd-2 after exposure to ethylene for 24 h.

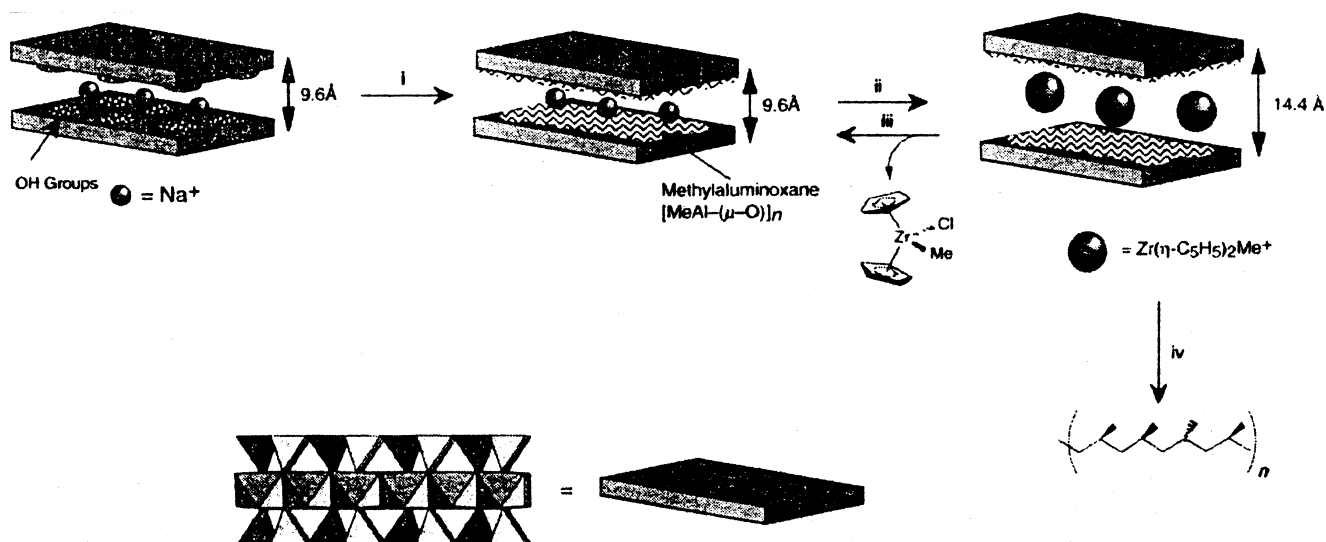


Fig. (2). Formation of PP/MMT nanocomposites under the catalysis of metalocene complex.

(MeGlyH⁺) [27], L-amino acids (AAH⁺Cl) or their methyl esters (MeAAH⁺Cl) [41] were effective in the exfoliation of MMT during ethylene homopolymerization or copolymerization with other olefins. Trimethylaluminum-depleted methylaluminoxane was used to modify MMT before a Ti-based constrained geometry catalyst was anchored to produce exfoliated PE nanocomposite (MMT loading up to 3.4 wt %) [39].

Alkylaluminum and vinylalcohol as bifunctional modifiers afforded vinyl groups chemically linked to the silicate surface which were copolymerized with ethylene inside the clay galleries using a nickel LTM catalyst [43]. Complete exfoliation of montmorillonite during Ti-based Ziegler-Natta polymerization of ethylene had been successfully carried out by using montmorillonite (MMT-OH) modified with intercalation agents containing hydroxyl groups. Hydroxyl groups in intercalation agents offered facile reactive sites for anchoring catalysts in between silicate layers although the polymerization activities significantly lowered due to the existence of hydroxyl groups [16]. PP/clay nanocomposites were prepared under Ziegler-Natta catalysis of propylene by way of ion exchanging the clay with an olefinic functionalized surfactant containing a chain end polymerizable double bond (Fig. 3) [22]. PE nanocomposites were prepared by *in-situ* polymerization method using the Ziegler-Natta catalyst supported on the OMMT/MgCl₂ bisupport in the presence of TEA as the cocatalyst [20].

Montmorillonite/silica hybrid (MT-Si) support was developed from CTAB-modified MT with expanding interlayer spacing (3.2 nm) due to *in situ* generated silica nanoparticles between galleries of the MT. Cp₂ZrCl₂ was fixed on the MT-Si surface and two classes of nanofillers (clay layers and silica nanoparticles) were dispersed concurrently in the PE matrix and exfoliated PE/clay-silica nanocomposites were obtained [30]. MMT/MgCl₂/TiCl₄ precatalyst was prepared by first diffusing MgCl₂ into the swollen MMT layers, followed by loading TiCl₄ on the inner/outer layer surfaces of

MMT where MgCl₂ was already deposited. The precatalyst upon activation with TEA polymerize ethylene to exfoliated PE nanocomposite with MMT loading below 1.0 wt % [17]. Polyethylene-clay nanocomposites were synthesized by *in situ* polymerization with 2,6-bis[1-(2,6-diisopropylphenylimino)ethyl] pyridine iron(II) dichloride supported on a modified montmorillonite clay pretreated with MAO [40]. However, the MMT loadings were limited to *ca.* 1.0 wt % in order to obtain exfoliated PE nanocomposites as indicated by wide-angle X-ray diffraction (WAXD) analyses. Nickel α -diimine LTM catalyst could be supported on the AlEt₃-activated OMMT and initiate ethylene polymerization to form PE/MMT nanocomposites which show reduced *d*₀₀₁ value (lower than that of OMMT) as the MMT loading reached 11.9 wt % [41].

OMMT-intercalated *rac*-Et(Ind)₂ZrCl₂ copolymerized ethylene and 10-undecen-1-ol with MAO the activator to form PE/MMT nanocomposites with comparable catalytic activities [34]. Taking similar route, *p*-methylstyrene (*p*MSt) was introduced to PE matrix which claimed to obtain structurally stable PE/MMT nanocomposites (Fig. 4) [36]. The copolymerization of propylene and 5-hexenyl-9-borabicyclo [3.3.1]nonane (5-hexenyl-9-BBN) catalyzed by OMMT-supported MgCl₂/TiCl₄/TEA-diphenyldimethoxysilane (DDS) resulted in exfoliated PP/MMT nanocomposites with reactive borane groups in the PP matrix [21].

Although details on the chemical substances are not disclosed, the organoclay precursors were made by ion exchanging clays with selected amine complexes capable of activating metallocene olefin polymerization catalysts. The as-modified clay powder was suspended in toluene and then mixed with hydrolytic scavengers and a highly isotactic metallocene propylene polymerization catalyst to produce PP-clay nanocomposites of various clay loadings by just changing the polymerization time [26]. For the PE/MMT nanocomposites from OMMT-Cp₂ZrCl₂ system, an increase of up to 25 °C in decomposition temperature is obtained whereas

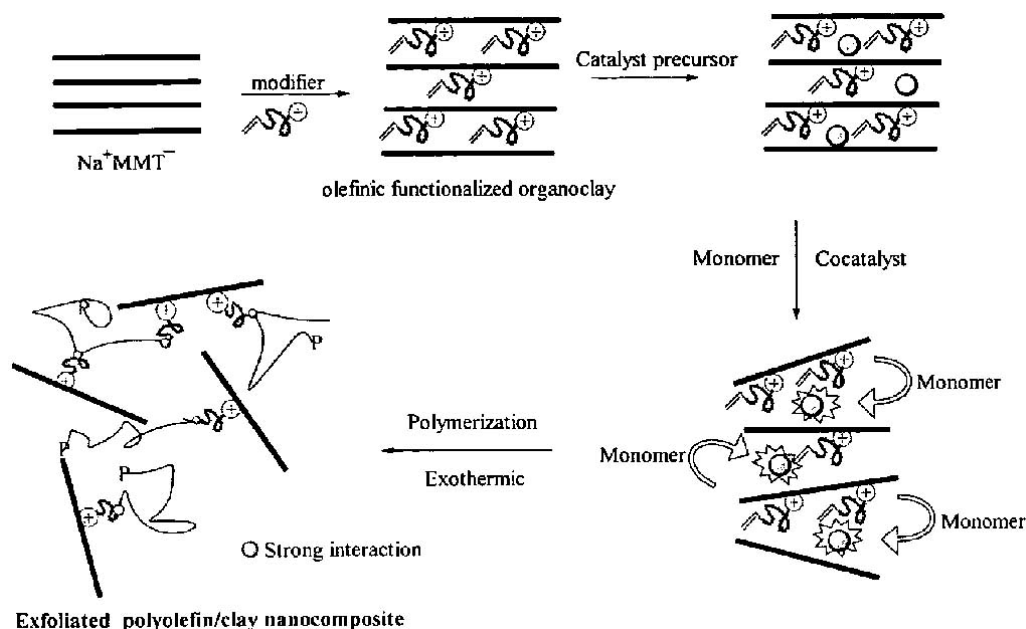


Fig. (3). Schematic illustration of a process for making polyolefin/clay nanocomposites using olefinic functionalized organoclay.

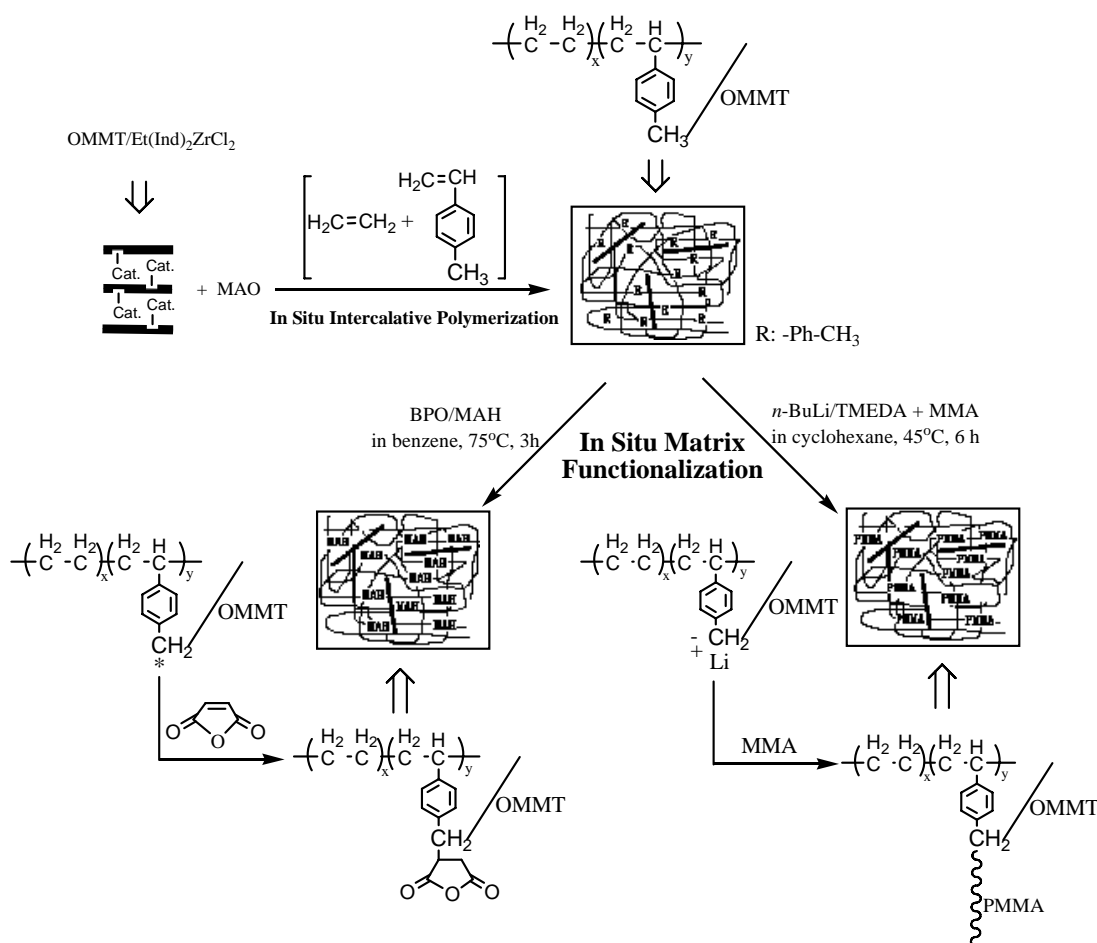


Fig. (4). Preparation route to PE-co-p-MS/OMMT nanocomposite and subsequent *in situ* matrix functionalization.

no much improved melting temperatures was resulted [32]. Using stearyl trimethyl ammonium chloride (SAC) as the swelling agent, an organo-MMT (OMMT) was resulted from the reaction of MMT with SAC and concentrated orthophosphoric acid. The OMMT reacted with a *rac*-Et(Ind)₂ZrCl₂ solution in toluene and MAO solution in toluene to form the supported catalyst [33]. (2-hydroxyethyl) hexadecyl diethylammonium iodine modified MMT reacted with excessive MAO and *rac*-Me₂Si(2-Me-4-Ph-Ind)₂ZrCl₂ to form MMT-supported catalyst together with external MAO and realized fairly high activities for propylene polymerization in the preparation of *i*-PP/MMT nanocomposite [37].

Totally different from other methods in synthesizing PE/MMT nanocomposites, tandem catalysis was subtly introduced to prepare PE/MMT nanocomposites by simply immobilizing precatalysts for ethylene oligomerization onto MMT and forming a dual functional catalytic system with homogeneous ethylene copolymerization catalysts [23, 24, 35, 38]. Due to the confinement effect of MMT's layered structure, significantly improved selectivity for low molar mass α -olefins were resulted from ethylene oligomerization, that, under the catalysis of another catalyst, metallocene complexes in general, *in situ* copolymerized with ethylene to manufacture PE/MMT nanocomposites with good activities in which the polymer matrix was linear low density polyethylene (LLDPE).

2. Structure Characterization of Polyolefin/Clay Nanocomposites

Wide angle X-ray diffraction (WAXD) and transmission electron microscopy (TEM) are major conventional tools in characterizing the structure of clay and polyolefin/clay nanocomposites with regard to the dispersion, intercalation, and exfoliation of clay and the resulting POE nanocomposites. In practice, WAXD and TEM are employed in combination to reflect the real state of clay layers.

Bragg Law ($n\lambda = 2d\sin\theta$) is used in calculating the interlayer spacing (d_{001}) of MMT according to the results from WAXD measurement. WAXD possesses the advantages of simple and rapid operation. The microstructure of the clay can be preliminarily determined in accordance with the position and intensity of the characteristic diffraction peak of clay. Also known from WAXD is the incompatible dispersion structure on micro scale, and intercalated or exfoliated structures on nano scale. Moreover, WAXD technique is a useful tool in studying the kinetics of the melt intercalation compounding process in producing polymer/clay nanocomposites.

It must be noticed that WAXD does not always present trustworthy information about the true structure of the nanocomposite materials when low clay loadings, e.g., < 2 wt %, occur. The absence of the characteristic diffraction peak in

this case does not represent complete exfoliation of clay. It is the sensitivity of WAXD and relatively weak diffraction intensity that lead to the undetectable signal. The reality might be the existence of an intercalated structure or even, in extreme cases, no dispersion of clay layers at all. On the other hand, WAXD presents statistical results of the samples, the actual space distribution and structural inhomogeneity of clay in the polymeric matrix are hardly reflected. In particular, it is difficult to make difference between partial exfoliation and partial intercalation. Also hard to determine is the relationship between the broadening of the characteristic diffraction peak plus the lowering of diffraction intensity and quantitative data in structural change.

As a direct means of observation, TEM discloses the internal layered structure of clay, the dispersion states of intercalated clay and exfoliated clay in polymer matrix, the space distribution, orientation and structural defect etc. of different phases. Disadvantages arising from using TEM lie in two points. One is the difficulty in sample preparation, the other is the time-dependence of the observation. Some polymer composites, like LLDPE/MMT nanocomposites, suffered from structural deterioration in very short time under the radiation of electron beams at high operating voltage. Fig. (5) depicts the WAXD patterns and TEM images of typical intercalated [37] and exfoliated [19] POE/MMT nanocomposites from olefin polymerization.

To make up what WAXD fails to fulfill, such as proofs of detailed structure on larger scale (e.g., d_{001} above 6 nm in intercalated nanocomposites or ordered structure in exfoliated nanocomposites), small angle X-ray scattering (SAXS) and neutron scattering turn to be powerful alternatives. Moreover, 2D WAXD and 2D SAXS can be utilized in probing structure and orientation on large scale. Solid NMR technique is also useful in obtaining clay morphology, surface chemistry, and, in particular, the process kinetics and degree of exfoliation of the nanocomposites. FT-IR and Raman spectroscopy are also used to analyze the structure of polyolefin/clay nanocomposites.

3. Properties of Polyolefin/Clay Nanocomposites

In general, polyolefin/clay nanocomposites exhibit improved comprehensive properties whichever fabrication methods are adopted. With the progress of research on the PE/clay nanocomposites, extensive investigation on more and more properties of the nanocomposites is conducted. The immobilization of pre-catalysts for olefin polymerization on clay usually increased the molecular weight of matrix polyolefins while narrower polydispersities were still maintained [12, 19, 25, 27, 30]. For example, the M_n s of PP from $Zr(\eta-C_5H_5)_2Cl_2$ and LaponiteRD-MAO- $Zr(\eta-C_5H_5)_2Me^+$ were 863 and 1996 $g\ mol^{-1}$, respectively, whereas the polydispersities were 2.4 and 1.9, respectively [12].

Using a magnesium based catalyst, very high catalyst efficiency was reached ($14650\ kg\ PE\ (mol\ Ti\ h)^{-1}$) for kaolin filler [13]. Whatever the investigated Al/Ti/Mg composition, the melting temperature (T_m) of the PE matrix is *ca.* 137 °C, except for one sample whose filler content was higher than all the other samples. Similarly, the crystallinity degree was basically independent of the catalyst composition. The melt viscosities were expectedly high in relation to a high filler content although the kaolin used in this case was indeed an anisotropic flake-like filler known for a drastic increase in the melt viscosity.

The filler particles were firstly coated by the growing PE chains, followed by the interconnection of the near neighbor particles through PE threads (Fig. (6)), thus increasing the mechanical strength of the composites due to improved compatibility between the polymer and the filler [13]. The superiority of polymerization-filled composites (PFCs) over melt-blended composites emerges from the comparison of the impact energy (*I.E.*), the elongation at rupture (ϵ_r), and the σ_{rc}/σ_{yc} tensile strength ratio [13]. With regard to an inorganic fiber, palygorskite, both the tensile strength and elongation at break were much lower for polyethylene/palygorskite nanocomposites prepared by *in situ* polymerization compared to the composites from melt blending

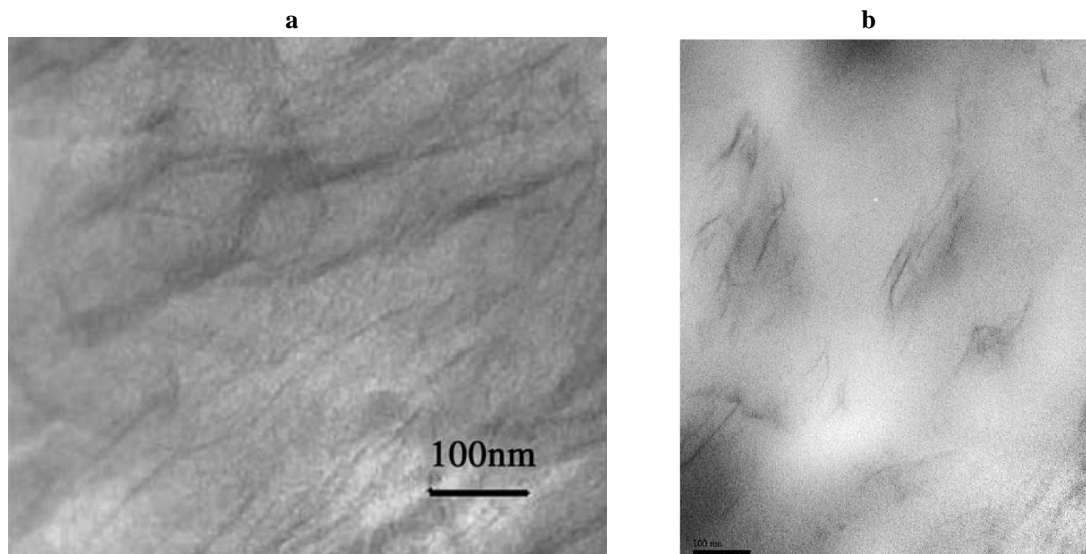


Fig. (5). TEM images of (a) intercalated *i*-PP/OMMT-OH_{0.8} nanocomposite containing 6.69 wt % of MMT; and (b) exfoliated PP/MMT nanocomposite containing 1.53 wt % of MMT.

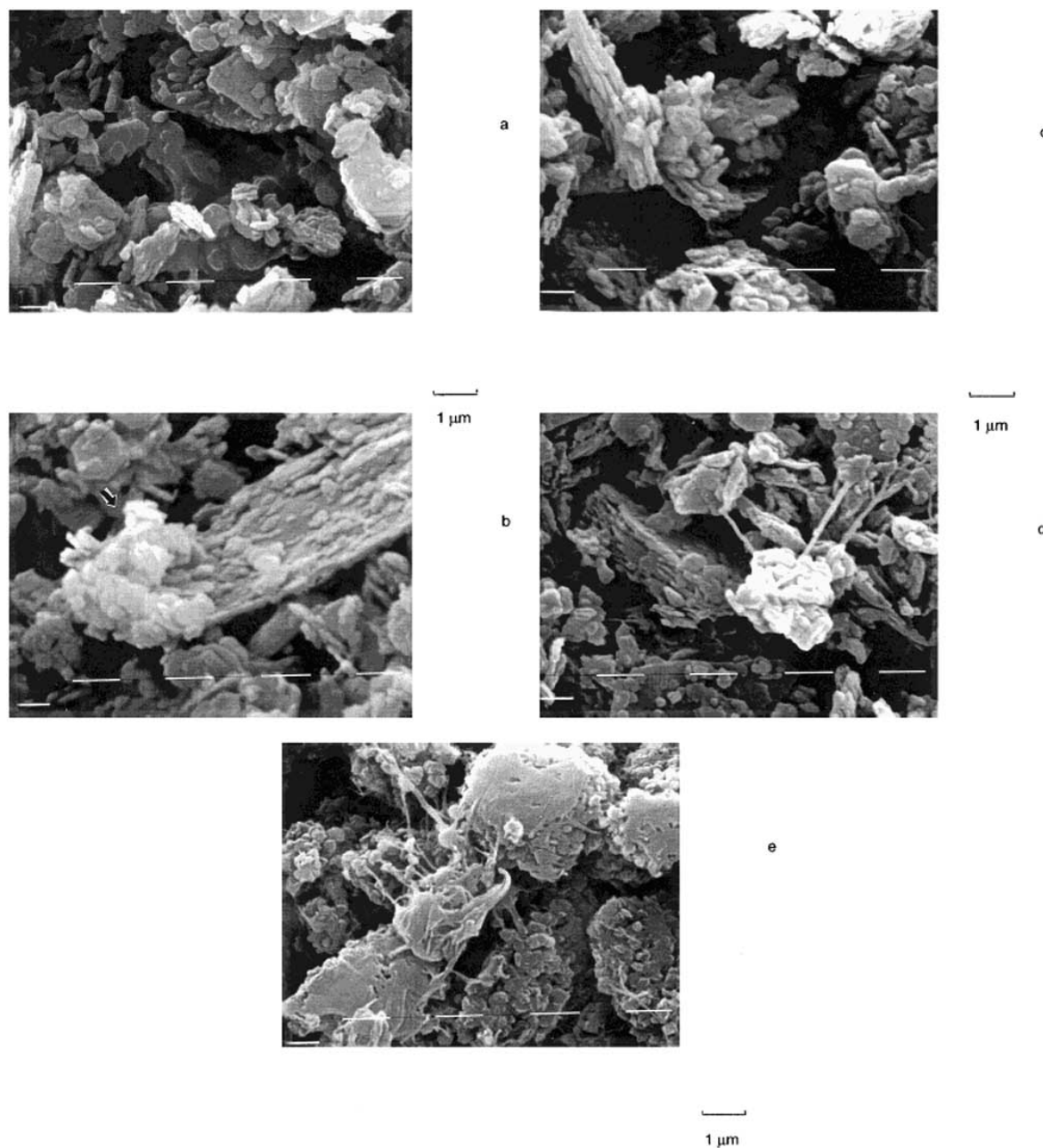


Fig. (6). SEM images of HDPE growing on the surface of kaolin Satintone W/W. HDPE content = (a): 0 wt %; (b): 10 wt %; (c): 20 wt %; (d): 30 wt %; and (e): 68 wt %.

due to poor bonding between polyethylene and palygorskite [14].

PP/MMT nanocomposites from MMT-supported Ziegler-Natta catalyst showed great increase in the dynamic storage modulus (E') especially at temperatures above the glass transition temperature (T_g) while the T_g s also rose in comparison to neat PP. Young's modulus of the nanocomposites found significant increment with MMT loadings. For the MMT loading of 2.5 wt %, relatively higher tension strength and elongation at break were observed. Also improved markedly is the T_{onset} (up 44 °C, MMT = 10.4 wt %) and HDT (up 40 °C, MMT = 8.1 wt %) for the nanocomposites. All of these

improvements arose from dispersion of MMT layers on nanoscale in PP matrix (Fig. 7) [15].

MMT-OH containing methyl tallow bis(2-hydroxyethyl) quaternary ammonium could be exfoliated with PE like a stretched accordion fold [16]. Meanwhile, the PEMMT-OH experienced stacking recovery after processing (extrusion) caused more serious stacking recovery than compression), which may be also a common phenomenon for other polyolefin/clay nanocomposites. The confinement of the nano-dispersed MMT layers to molecular chain and the strong interaction between the nanoscale MMT layers and the resin matrix were thought to account for the decrease of crystallin-

ity and the remarkable enhancement of tensile strength of PE/MMT nanocomposites prepared by *in situ* coordination polymerization using a MMT/MgCl₂/TiCl₄ catalyst activated by TEA [17].

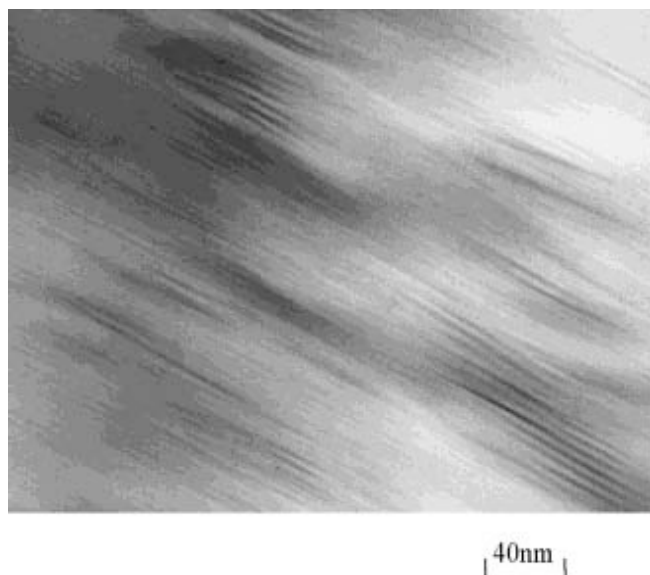


Fig. (7). TEM images of PP/MMT nanocomposites.

MMT modified with alkyl-imidazolium (IMMT), alkylammonium (AMMT), and alkyltriphenylphosphonium (PMMT) behaved differently with regard to the thermal stability of PP/MMT nanocomposites with IMMT featuring the highest T_{max} of 422 °C [18, 19]. With the increase of the organoclay loading, the number of degradation stages decreased. Meanwhile, the presence of the exfoliated clay nanolayers increased the E_a of the thermo-oxidative degradation process of the PE matrix as indicated by improved thermal oxidation stability [28].

A low degree of hydroxyl functionalization of PE, e.g., 0.16 mol % of hydroxyl groups in PE for a 5.36 wt % of OMMT filling, showed remarkable structure-stabilizing effect when the as-prepared PE/OMMT nanocomposites were subjected to thermal processing [34]. In contrast, the compression-molding of PE/MMT nanocomposite significantly affected the original dispersion of the clay layers in the polyethylene matrix and caused stacking recovery possibly because of the transformation of interlayer structure from bilayer arrangement to monolayer arrangement, which make the surface character of the organoclay less organophilic [41]. In contrast to the heterogeneous catalysts on kaolin, heterogeneous catalysts formed on MMT were very active in ethylene and propylene polymerization while *rac*-Et(Ind)₂ZrCl₂ was used [25]. Moreover, values of the melting temperature and tacticity regarding PP significantly decreased compared to the case of employing homogeneous *rac*-Et(Ind)₂ZrCl₂.

The molecular weight of these PP-clay nanocomposites could be controlled by the polymerization temperature and monomer concentration in the polymerization slurry. The isotacticity of the PP matrix varied over a very narrow range, typically from 95-98 %, as determined by ¹³C NMR. Also realized in this case is the drastically improved Young's ten-

sile modulus, up to 600 kpsi, which is well above the modulus of highly crystalline PP. Other improved properties of the PP/clay nanocomposites made in this work are reduced thermal expansion coefficient, improved melt flow strength, increased HDT, and lowered gas diffusion coefficient [26]. In addition to high loadings of Zr, Cp₂ZrCl₂ supported on MeGlyH⁺-modified MMT also (co)polymerized ethylene to PE/MMT nanocomposites with good bulk density (in most cases > 0.3 g cm⁻³) [27]. Similar results are obtained with other modifiers like AAH⁺Cl⁻ or (MeAAH⁺Cl⁻) when such metallocene was used in ethylene (co)polymerization to form PE/MMT nanocomposites [28].

PE/MMT composites from ethylene catalysis over (*n*-BuCp)₂ZrCl₂ fixed on MAO-treated MMT reveal that different polyethylenes were generated before and after delamination of the silicate layers as reflected by XRD and DSC analyses [29]. Meanwhile, the layered structure of clay also affected the polymerization reactions, especially chain transfer and termination reaction, which influenced the molecular weight of polymer.

rac-Et(Ind)₂ZrCl₂ supported on SAC-treated MMT produced PP/MMT nanocomposites represented by the coexistence of intercalation and exfoliation of MMT layers upon polypropylene polymerization. PP/MMT nanocomposite had more [mmmm] pentads so that the PP/MMT nanocomposite had a higher T_m and ΔH than PP under the same reaction conditions. As evidenced by improved HV values (Vicker hardness), the silicate sheets of MMT could provide good hardness property in the as-prepared composite [33].

As elucidated by SEM observation, the shape of the pure PP particles resembled that of the *rac*-Et(Ind)₂ZrCl₂ catalyst, as depicted in Fig. (8a,b). The particle sizes were about 4–6 μm at a reaction temperature of 40 °C but the PP particles fragmented into smaller particles at higher reaction temperatures (Fig. 8a,b). The shapes of PP/MMT nanocomposites differed completely from those of PP, as shown in Fig. (8c,d). The larger particles of PP/MMT particles were obtained by the *rac*-Et(Ind)₂ZrCl₂-supported catalyst and the diameters of the particles were estimated in the range of 10–30 μm. Larger particles increase the bulk density of the PP/MMT nanocomposite. Additionally, the bulk density of PP/MMT nanocomposites clearly increased with the MMT content [33].

A reactive PE matrix bearing *p*-MS units was capable of undergoing free radical and butyllithium-induced maleation reactions under mild reaction conditions with the latter being followed by an anionic graft-from polymerization of MMA. It's the pendant maleic anhydride groups and the polar PMMA side chains that effectively improved the miscibility between the PE matrix and delaminated MMT layers, leading to significant stability enhancement of the nanocomposite structure against processing (Fig. 9).

The existence of silica nanoparticles in the galleries of C16-MT played a very important role in the preparation of well dispersed PE nanocomposites from metallocene catalysis. When MT-Si-cat is used (S1–6), high tensile moduli (1665 MPa) and dynamic storage moduli were observed. Little improvement in tensile strength was also observed for samples S1–6. Noticeably, it is not possible to compare the samples (S0–8) directly because the filler content and the PE

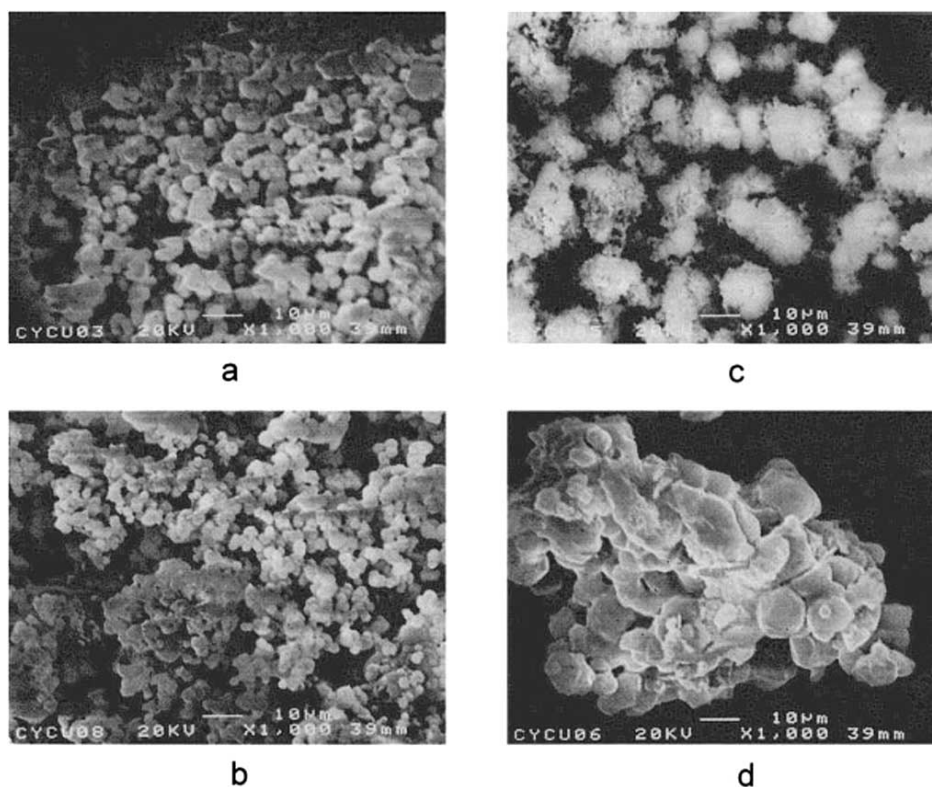


Fig. (8). SEM photographs of PP at (a) 40 °C (P-1); (b) 80 °C (P-2); and PP/MMT nanocomposite at (c) 40 °C (PCH-4); (d) 80 °C (PCH-5).

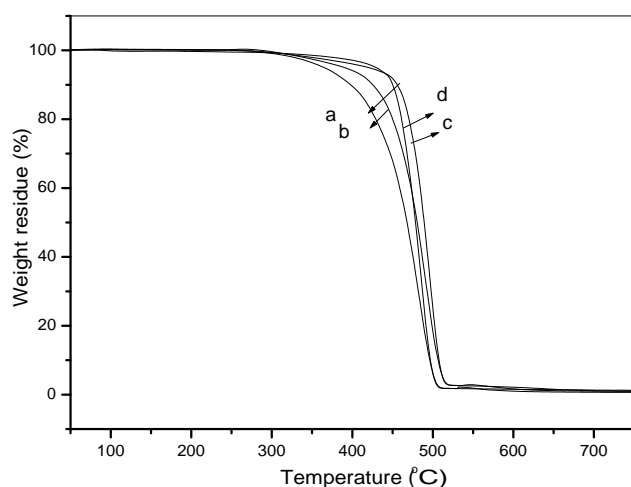


Fig. (9). TGA curves of samples (a) as-polymerized; (b) compression-molded; (c) MA-functionalized; and (d) PMMA-functionalized PE-co-p-MS/OMMT nanocomposites containing 0.90 mol% of p-MS units and 1.5 wt % of OMMT.

molecular weight change at random. Additionally, sample S0 produced with homogeneous catalyst showed a spongy structure with a low bulk density of 0.07 g cm^{-3} , whereas sample S1 presented a granular morphology with a bulk density of 0.2 g cm^{-3} , typical of a heterogeneous catalyst system, indicating that the supported catalyst MT-Si-cat is applicable to slurry processes [30].

(3-Aminopropyl)triethoxysilane (APTEOS)/MAO-modified MMT intercalated by Cp_2ZrCl_2 produced PE (in fact (nano)composites with MMT although it's not the focus of

this work) of bimodal molecular weight distribution possibly due to different reaction modes between APTEOS and pre-treated MMT which resulted in MMT-7 with two distinct interlayer spacings (2.08 and 1.10 nm, resp.) [31]. So the pretreatment of MMT had a significant influence on the interlayer structures of the resulting modified MMTs due to differences in the chemical and physical environment of specific catalytic sites as confirmed by XRD and XPS characterization. This will further affect the anchorage of approaching zirconocene compounds. With regard to ethylene copolymerization with oct-1-ene using similar catalysts, PEs produced by the supported catalyst had lower average M_w and broader MWD than those by homogeneous catalyst. The average M_w and melting temperature (T_m) of the polymers produced in ethylene homopolymerization were higher than those in copolymerization [31]. Finally, branching from oct-1-ene insertion was more favorable for MMT-supported Cp_2ZrCl_2 with different interlayer spacings than for its homogeneous analogue.

Metallocene-catalyzed ethylene homo- and copolymerization in the presence of organophilic layered silicates (bentonites and hectorites) afforded PE nanocomposites with improved stiffness and strength with respect to those obtained for melt-compounding nanocomposites [44]. Additionally, oct-1-ene incorporation appeared to improve compatibility between polyethylene and modified silicates. However, the precatalysts in this case were not tethered onto layered silicates. (2-hydroxyethyl) hexadecyl diethylammonium iodine exchanged with MMT to afford reactive OH groups on the surface of MMT layers. PP/MMT nanocomposites from propylene polymerization catalyzed by $\text{rac-Me}_2\text{Si}(2\text{-Me-4-Ph-Ind})_2\text{ZrCl}_2$ that was immobilized on the

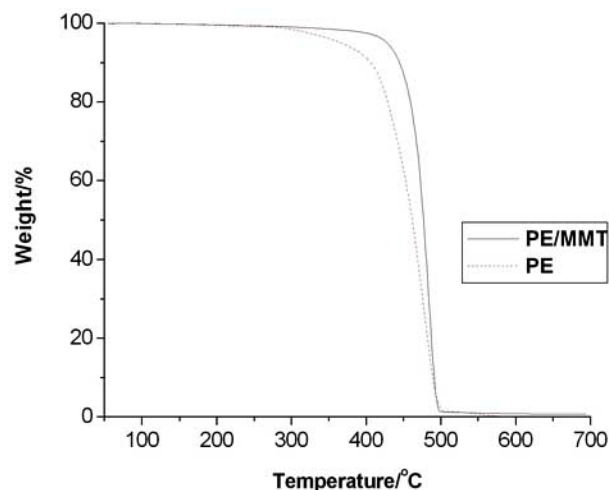


Fig. (10). TGA traces of PE and PE/MMT nanocomposite containing 3.0 wt % of MMT.

as-prepared OMMT exhibited improved thermal stability while high molecular weights of the polymer matrix were maintained [37]. Unfortunately, no results were reported as to changes in the isotacticity of PP produced in this case.

Similar results were obtained from ethylene polymerization catalyzed by CGC and MAO pretreated kaolin [39]. An increase in the nanofiller content clearly resulted in a dramatic increase in crystallinity, parallel to a higher T_m , which suggested a nucleating activity of the nanofiller. In the case of PE of lower molecular weight, the storage moduli drastically rose with hectorite loadings [39]. Three transitions observed at ca. -115, -25, and 70 °C could be assigned to the γ , β , and α relaxations of PE, respectively. All these relaxations changed with the filler content, suggesting that the nanofillers influenced not only the properties of the amorphous polyethylene but also the crystalline regions [39].

Quite different from other synthetic routes to PE/MMT nanocomposites, the concept of copolymerization of ethylene with *in situ* generated α -olefins also proved to be a highly effective method [23, 24, 35, 38]. This method combined the advantages of linear low density polyethylene (LLDPE) and highly uniform dispersed MMT layers throughout the LLDPE matrix. In addition to completely exfoliated structure of MMT sheets, greatly improved thermal stability was realized as well (Fig. 10). More strikingly, all of the as-prepared PE/MMT nanocomposites showed remarkable improvement in tensile strength and Young's modulus while their elongation at break decreased. Moreover, the flexural strength of the PE/MMT nanocomposites increased by 2-3 times with the flexural modulus maintained at their original levels (Fig. 11) [38].

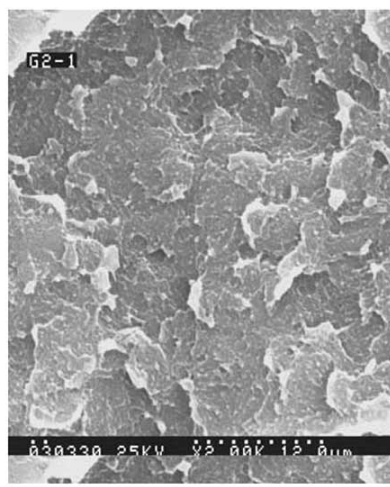
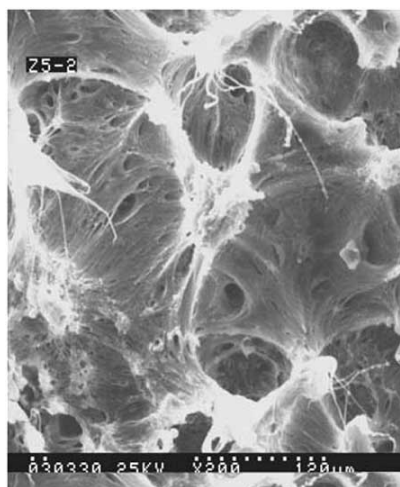
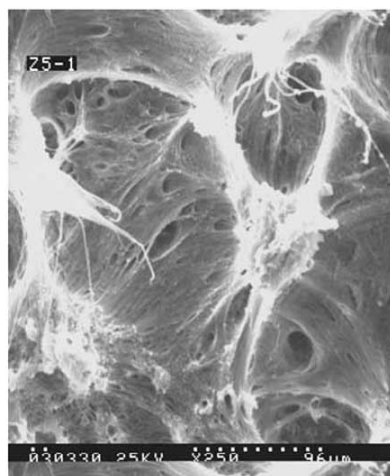
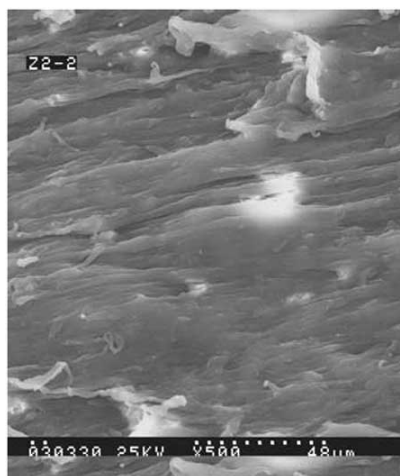


Fig. (11). Contd.....

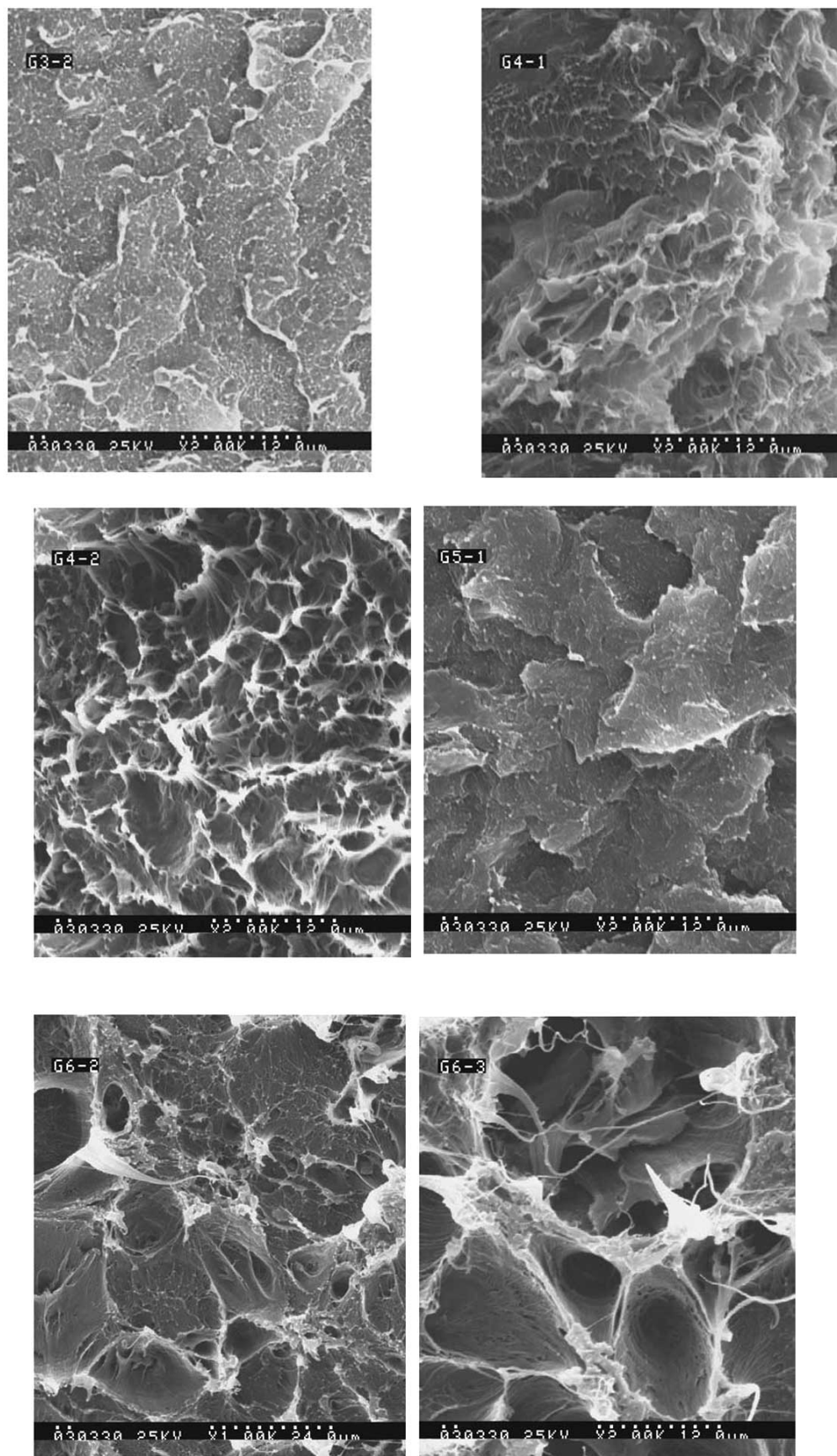


Fig. (11). Morphology of cross section of PE and PE/MMT nanocomposites.

Up to now, there has been a little research on the crystallization of polyolefin/MMT nanocomposites prepared by olefin polymerization methods [20, 45]. Highly uniform dispersion MMT nanolayers invariably increase the crystallization rate and crystallization temperature due to the heterogeneous nucleating role of dispersed MMT particles. These effects ensured rapid crystallization for practical applications (Fig. 12) [45].

4. Outlook for Future Development in Polyolefin/Clay Nanocomposites

As has been described above, polyolefin/clay nanocomposites preparation *via* olefin (co)polymerization present itself a promising method in fabricating polyolefin nanocomposites with drastically improved chemical and physical properties. With continued efforts of numerous researchers,

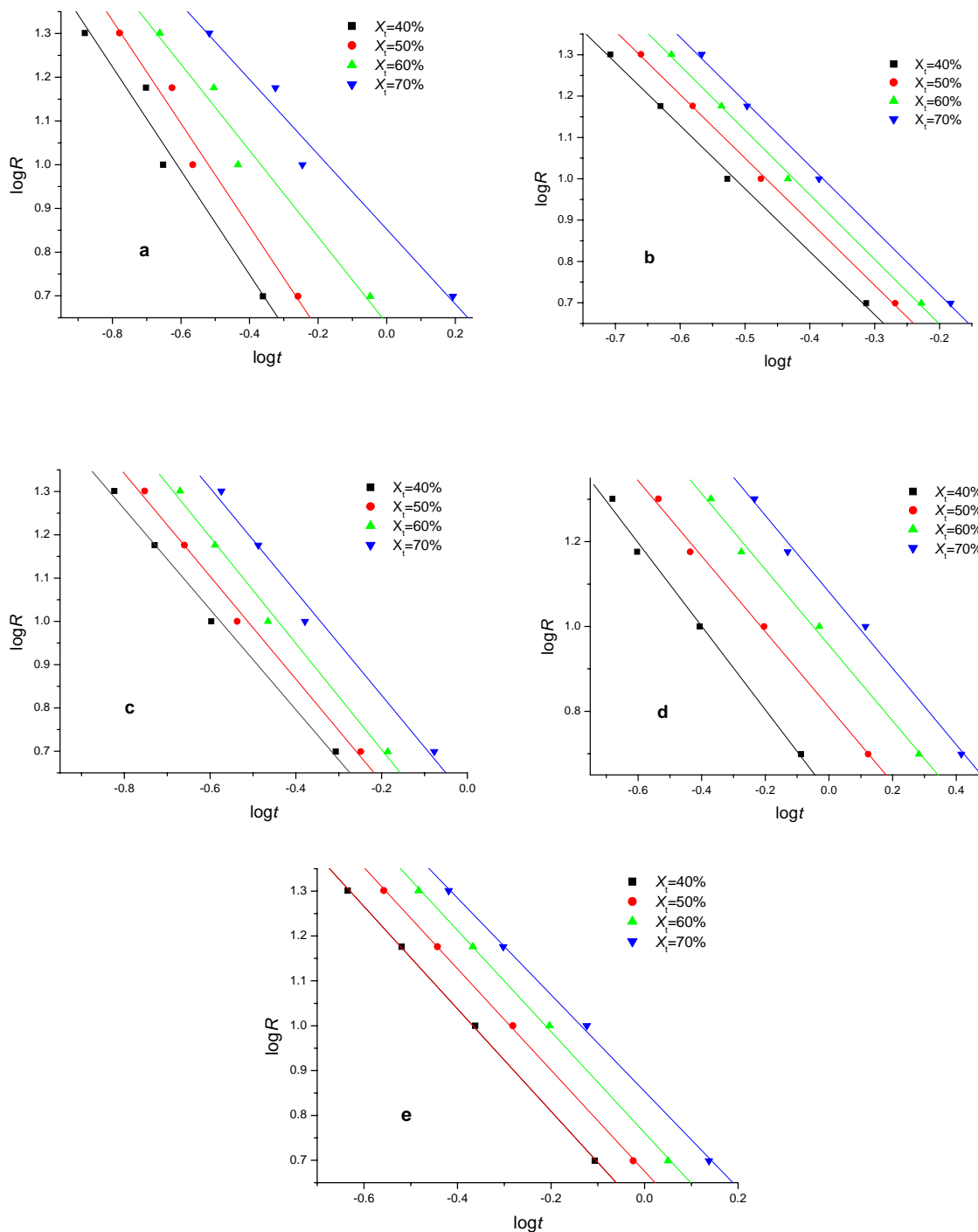


Fig. (12). Curves of $\log R$ vs $\log t$: (a) PE; (b) PE/MMT1 (MMT = 0.2 wt %); (c) PE/MMT2 (MMT = 1.0 wt %); (d) PE/MMT3 (MMT = 2.4 wt %); (e) PE/MMT4 (MMT = 4.0 wt %).

the as-prepared nanocomposites of MMT loadings below 5 wt % are advantageous in preserving an exfoliated structure. However, the polyolefin matrix and the MMT layers already dispersed tend to form phase separation upon thermal or mechanical processing. Usually, an MMT loading below 2 wt % is better for realizing stable nano-structure of the composites.

To make the present polymerization-induced formation of polyolefin/clay nanocomposites applicable to industrial bulk or slurry processes, more efforts are needed with regard to the preparation of regular morphology of catalytic species, prevention against re-aggregation or stacking recovery of the already intercalated or exfoliated MMT sheets, and the rheological properties of the nanocomposites with various structures and different MMT loadings.

As a result, the key issue in further developing such a polymerization method is the search for a good balance among catalytic efficiency, morphology control, phase stability, and property adjustment.

ACKNOWLEDGEMENT

We acknowledge the funding from the National Natural Science Foundation of China (NSFC, Nos. 50103012, 20774100).

REFERENCES

- Wheeler, A. Vapor-phase polymerization of tetrafluoroethylene. US 2847391 1958.
- Okada, A.; Kawasumi, M.; Kurauchi, T.; Kamigaito, O. Synthesis and characterization of a nylon 6-clay hybrid. *Polym. Prepr.*, **1987**, *28*, 447-448.
- Kawasumi, M.; Hasegawa, N.; Kato, M.; Usuki, A.; Okada, A. Preparation and mechanical properties of polypropylene-clay hybrids. *Macromolecules*, **1997**, *30*, 6333-6338.
- Lee, J.W.; Lim, Y.T.; Park, O.O. Thermal characteristics of organoclay and their effects upon the formation of polypropylene/organoclay nanocomposites. *Polym. Bull.*, **2000**, *45*, 191-198.
- Wang, K.H.; Xu, M.Z.; Choi, Y.S.; Chung, I.J. Effect of aspect ratio of clay on melt extensional process of maleated polyethylene/clay nanocomposites. *Polym. Bull.*, **2001**, *46*, 499-505.
- Wang, K.H.; Cho, M.H.; Koo, C.M.; Xu, M.Z.; Chung, I.J.; Jang, M.C.; Choi, S.W.; Song, H.H. Morphology and physical properties of polyethylene/silicate nanocomposite prepared by melt intercalation. *J. Polym. Sci. Part B: Polym. Phys.*, **2002**, *40*, 1454-1463.
- Wang, K.H.; Chung, I.J.; Jang, M.C.; Keum, J.K.; Song, H.H. Deformation behavior of polyethylene/silicate nanocomposites as studied by real-time wide-angle X-ray scattering. *Macromolecules*, **2002**, *35*, 5529-5535.
- Furuichi, N.; Kurokawa, Y.; Fujita, K.; Oya, A.; Yasuda, H.; Kiso, M. Preparation and properties of polypropylene reinforced by smectite. *J. Mater. Sci.*, **1996**, *31*, 4307-4310.
- Kurukawa, Y.; Yasuda, H.; Kashiwagi, M.; Oya, A. Structure and properties of a montmorillonite/polypropylene nanocomposite. *J. Mater. Sci. Lett.*, **1997**, *16*, 1670-1672.
- Jehon, H.G.; Jung, H.T.; Lee, S.W.; Hudson, S.D. Morphology of polymer/silicate nanocomposites. *Polym. Bull.*, **1998**, *41*, 107-113.
- Hudson, S.D. Polyolefin nanocomposites. US 5910523 1999.
- Tudor, J.; Willington, L.; O'Hare, D.; Royan, B. Intercalation of catalytically active metal complexes in phyllosilicates and their application as propene polymerization catalysts. *Chem. Commun.*, **1996**, 2031-2032.
- Hindryckx, F.; Dubois, P.; Jerome, R.; Teyssie, P.; Marti, M.G. Polymerization-filled composites prepared with highly active filler-supported Al/Ti/Mg catalysts. II. Properties of homogeneous polyethylene-based composites. *J. Appl. Polym. Sci.*, **1997**, *64*, 439-454.
- Rong, J.F.; Jing, Z.H.; Li, H.Q.; Sheng, M. A polyethylene nanocomposite prepared via *in-situ* polymerization. *Macromol. Rapid Commun.*, **2001**, *22*, 329-334.
- Ma, J.; Qi, Z.; Hu, Y. Synthesis and characterization of polypropylene/clay nanocomposites. *J. Appl. Polym. Sci.*, **2001**, *82*, 3611-3617.
- Jin, Y.H.; Park, H.J.; Im, S.S.; Kwak, S.Y.; Kwak, S. Polyethylene/clay nanocomposite by *in-situ* exfoliation of montmorillonite during Ziegler-Natta polymerization of ethylene. *Macromol. Rapid Commun.*, **2002**, *20*, 135-140.
- Yang, F.; Zhang, X.Q.; Zhao, H.C.; Chen, B.; Huang, B.T.; Feng, Z.L. Preparation and properties of polyethylene/montmorillonite nanocomposites by *in situ* polymerization. *J. Appl. Polym. Sci.*, **2003**, *89*, 3680-3684.
- He, A.H.; Hu, H.Q.; Huang, Y.J.; Dong, J.Y.; Han, C.C. Isotactic poly(propylene)/ monoalkylimidazolium-modified montmorillonite nanocomposites: preparation by intercalative polymerization and thermal stability study. *Macromol. Rapid Commun.*, **2004**, *25*, 2008-2013.
- He, A.H.; Wang, L.M.; Li, J.X.; Dong, J.Y.; Han, C.C. Preparation of exfoliated isotactic polypropylene/alkyl-triphenylphosphonium-modified montmorillonite nanocomposites via *in situ* intercalative polymerization. *Polymer*, **2006**, *47*, 1767-1771.
- He, F.A.; Zhang, L.M.; Yang, F.; Chen, L.S.; Wu, Q. Polyethylene nanocomposites obtained from *in-situ* polymerization using supported Ziegler-Natta catalyst system. *J. Macromol. Sci. A.*, **2007**, *44*, 11-15.
- Yang, K.F.; Huang, Y.J.; Dong, J.Y. Preparation of polypropylene/montmorillonite nanocomposites by intercalative polymerization: Effect of *in situ* polymer matrix functionalization on the stability of the nanocomposite structure. *Chin. Sci. Bull.*, **2007**, *52*, 181-187.
- Lu, H.; Liu, Z.; Chen, C.-J.; Hu, Y.; Lu, Y.; Ke, Y.; Guo, C. Process for making exfoliated polyolefin/clay nanocomposites, US 7432319B2 2007.
- Wang, J.; Liu, Z.Y.; Guo, C.Y.; Chen, Y.J.; Wang, D. Preparation of a PE/MT composite by copolymerization of ethylene with *in-situ* produced ethylene oligomers under a dual functional catalyst system intercalated into MT layer. *Macromol. Rapid Commun.*, **2001**, *22*, 1422-1426.
- Guo, C.Y.; Ma, Z.; Zhang, M.G.; He, A.H.; Ke, Y.C.; Hu, Y.L. Preparation of PE/MMT nanocomposite by monomer intercalation and *in situ* copolymerization. *Chin. Sci. Bull.*, **2002**, *47*, 1267-1270.
- Weiss, K.; Wirth-Pfeifer, C.; Hofmann, M.; Botzenhardt, S.; Lang, H.; Brüning, K.; Meichel, E. Polymerisation of ethylene or propylene with heterogeneous metallocene catalysts on clay minerals. *J. Mol. Catal. A: Chem.*, **2002**, *182-183*, 143-149.
- Sun, T.; Garcés, J.M. High-performance polypropylene-clay nanocomposites by *in-situ* polymerization with metallocene/clay catalysts. *Adv. Mater.*, **2002**, *14*, 128-130.
- Liu, C.B.; Tang, T.; Zhao, Z.F.; Huang, B.T. Preparation of functionalized montmorillonite and their application in supported zirconocene catalysts for ethylene polymerization. *J. Polym. Sci.: Part A: Polym. Chem.*, **2002**, *40*, 1892-1898.
- Liu, C.B.; Tang, T.; Wang, D.; Huang, B.T. *In situ* ethylene homopolymerization and copolymerization catalyzed by zirconocene catalysts entrapped inside functionalized montmorillonite. *J. Polym. Sci.: Part A: Polym. Chem.*, **2003**, *41*, 2187-2196.
- Wang, Q.; Zhou, Z.Y.; Song, L.X.; Xu, H.; Wang, L. Nanoscopic confinement effects on ethylene polymerization by intercalated silicate with metallocene catalyst. *J. Polym. Sci. Part A: Polym. Chem.*, **2004**, *42*, 38-43.
- Wei, L.M.; Tang, T.; Huang, B. Synthesis and characterization of polyethylene/clay-silica nanocomposites: A montmorillonite/silica-hybrid-supported catalyst and *in situ* polymerization. *J. Polym. Sci. Part A: Polym. Chem.*, **2004**, *42*, 941-949.
- Liu, C.B.; Tang, T.; Huang, B.T. Zirconocene catalyst well spaced inside modified montmorillonite for ethylene polymerization: role of pretreatment and modification of montmorillonite in tailoring polymer properties. *J. Catal.*, **2004**, *221*, 162-169.
- Lee, D.H.; Kim, H.S.; Yoon, K.B.; Min, K.E.; Seo, K.H.; Noh, S.K. Polyethylene/MMT nanocomposites prepared by *in situ* polymerization using supported catalyst systems. *Sci. Tech. Adv. Mater.*, **2005**, *6*, 457-462.
- Hwu, J.M.; Jiang, G.J. Preparation and characterization of polypropylene-montmorillonite nanocomposites generated by *in situ* metallocene catalyst polymerization. *J. Appl. Polym. Sci.*, **2005**, *95*, 1228-1236.

- [34] Huang, Y.J.; Yang, K.F.; Dong, J.Y. Copolymerization of ethylene and 10-undecen-1-ol using a montmorillonite-intercalated metallocene catalyst: Synthesis of polyethylene/montmorillonite nanocomposites with enhanced structural stability. *Macromol. Rapid Commun.*, **2006**, *27*, 1278-1283.
- [35] Qian, J.; Guo, C.-Y.; Wang, H.; Hu, Y. Fabrication and characterization of PE/MMT nanocomposites via copolymerization of ethylene and *in situ* formed α -olefins. *J. Mater. Sci.*, **2007**, *42*, 4350-4355.
- [36] Huang, Y.J.; Yang, K.F.; Dong, J.Y. An *in situ* matrix functionalization approach to structure stability enhancement in polyethylene/montmorillonite nanocomposites prepared by intercalative polymerization. *Polymer*, **2007**, *48*, 4005-4014.
- [37] Yang, K.F.; Huang, Y.J.; Dong, J.Y. Efficient preparation of isotactic polypropylene/montmorillonite nanocomposites by *in situ* polymerization technique via a combined use of functional surfactant and metallocene catalysis. *Polymer*, **2007**, *48*, 6254-6261.
- [38] Guo, C.-Y.; Ke, Y.; Liu, Y.; Mi, X.; Zhang, M.; Hu, Y. Preparation and property investigation of PE/MMT nanocomposites formed via ethylene copolymerization. *Polym. Int.*, **2009**, DOI: 10.1002/pi.2666.
- [39] Alexandre, M.; Dubois, P.; Sun, T.; Garcés, J.M.; Jérôme, R. Polyethylene-layered silicate nanocomposites prepared by the polymerization-filling technique: synthesis and mechanical properties. *Polymer*, **2002**, *43*, 2123-2132.
- [40] Ray, S.; Galgali, G.; Lele, A.; Sivaram, S. *In situ* polymerization of ethylene with bis(imino)pyridine iron(II) catalysts supported on clay: The synthesis and characterization of polyethylene-clay nanocomposites. *J. Polym. Sci. Part A: Polym. Chem.*, **2005**, *43*, 304-318.
- [41] He, F.-A.; Zhang, L.-M.; Jiang, H.-L.; Chen, L.-S.; Wu, Q.; Wang, H.-H. A new strategy to prepare polyethylene nanocomposites by using a late-transition-metal catalyst supported on AlEt₃-activated organoclay. *Comp. Sci. Tech.*, **2007**, *67*, 1727-1733.
- [42] Bergman, J.S.; Chen, H.; Giannelis, E.P.; Thomas, M.G.; Coates, G.W. Synthesis and characterization of polyolefin-silicate nanocomposites: a catalyst intercalation and *in situ* polymerization approach. *Chem. Commun.*, **1999**, 2179-2180.
- [43] Shin, S.Y.A.; Simon, L.C.; Soares, J.B.P.; Scholz, G. Polyethylene-clay hybrid nanocomposites: *in situ* polymerization using bifunctional organic modifiers. *Polymer*, **2003**, *44*, 5317-5321.
- [44] Heinemann, J.; Richert, P.; Thomann, R.; Mülhaupt, R. Polyolefin nanocomposites formed by melt compounding and transition metal catalyzed ethene homo- and copolymerization in the presence of layered silicates. *Macromol. Rapid Commun.*, **1999**, *20*, 423-430.
- [45] Shi, B.; Guo, C.-Y.; Ke, Y.; Zhang, M.; Hu, Y. Nonisothermal crystallization behavior of *in-situ* formed polyethylene/montmorillonite (PE/MMT) nanocomposites through ethylene copolymerization. *Open Macromol. J.*, **2009**, *3*, 6-11.

Received: August 17, 2009

Revised: October 30, 2009

Accepted: November 11, 2009

© Qian and Guo; Licensee Bentham Open.

This is an open access article licensed under the terms of the Creative Commons Attribution Non-Commercial License (<http://creativecommons.org/licenses/by-nc/3.0/>) which permits unrestricted, non-commercial use, distribution and reproduction in any medium, provided the work is properly cited.